VALIDATION OF A HDR-BASED DEVICE MODEL BY EXPERIMENTAL TESTS ON A STEEL-CONCRETE COMPOSITE FRAME

A. Dall'Asta[1], L. Dezi[2], G. Leoni[1] and L.Ragni[2]

[1] *Department ProCAm, University of Camerino, Ascoli Piceno, Italy*
[2] *DACS, Marche Polytechnic University, Ancona, Italy*

ABSTRACT :

High Damping Rubber (HDR), commonly used for seismic isolation devices, may also be used to produce passive dissipation devices. HDR-based devices have a number of advantages: they are recentering, they can withstanding a large number of cycle and moreover they can dissipate energy even under low excitations, such in the case of frequent earthquakes or wind actions. This paper presents a validation of a nonlinear viscoelastic model for HDR-based dampers already proposed by the same authors, by means of comparisons with experimental tests carried out on a full scale steel-concrete composite mock-up. The paper firstly describes the real scale mock-up and its characterization, in the elastic displacement range, carried out by means of free vibration tests. HDR devices were introduced in the frame by means of chevron-type braces and dynamic free vibration tests, force-controlled tests and displacement-controlled tests were performed. The coupled system is modelled as a nonlinear SDOF system consisting of an linear elastic element placed in parallel with HDR dampers. All experimental tests were numerically simulated with satisfactory results.

KEYWORDS: High Damping Rubber, dissipation devices, experimental tests, HDR model.

1. INTRODUCTION

Among passive dissipation devices currently applied in new and existing structures (Soong and Spencer 2002) those based on High Damping Rubber (HDR), commonly used to construct bearing devices, are of a certain interest due to their capacity in withstanding a large number of cycles and in recentering after deformation. Furthermore, the capacity in dissipating energy under low excitations, such in the case of frequent earthquakes or wind actions, makes their use attractive to control structural vibrations and damageability.
Scientific literature reports experimental tests on the material (Haupt 2001, Grant et al. 2005) and on single HDR bearings (Hwang et al. 2002, Tsai et al. 2003) and many numerical models which have been proposed on the basis of the test results. There are however very few studies (Fuller et al. 2000) dealing with experimental dynamic tests on structures equipped with HDR based dampers.
In Dall'Asta and Ragni (2006) the authors carried out relaxation tests and cyclic displacement-controlled tests on HDR-based devices in order to understand the behaviour of the material under shear loads. A suitable constitutive model was developed to simulate the non linear viscous-elastic behaviour of the device also characterised by interior damage (Mullins effect). By considering the rubber subjected to a generic time history of shear strains, the shear stress is evaluated by the relationship

$$\tau_0 = f_e(\gamma) + E_{v1}(\gamma - \gamma_{v1}) + E_{v2}(\gamma - \gamma_{v2}) + \alpha_m(1 - q_e) f_e(\gamma) + E_{v3}(1 - q_v)(\gamma - \gamma_{v3}) \qquad (1.1)$$

where the first term is a non linear elastic component, the second and third terms are nonlinear viscous-elastic components, and the last two terms are non linear components accounting for Mullins effect. The inelastic strains γ_{v1}, γ_{v2} and γ_{v3} and the damage parameters q_e and q_v are the internal variables of the model and may be grouped in the vector

$$\boldsymbol{\alpha}^T = [\gamma_{v1} \quad \gamma_{v2} \quad \gamma_{v3} \quad q_e \quad q_v] \qquad (1.2)$$

The behaviour of the rubber is thus described by the non linear evolution law

$$\dot{\boldsymbol{\alpha}} = \mathbf{A}(\gamma, \dot{\gamma}, \alpha) \tag{1.3}$$

not explicated here for the sake of brevity, but reported in Dall'Asta and Ragni (2006). Parameters E_{v1}, E_{v2}, α_m and E_{v3} appearing in Eqn. 1.1 and those contained in the evolution laws were determined from relaxation tests and strain-rate constant cyclic tests carried out on the device. The theoretical predictions are in good agreement with the experimental tests on the device. However the real ability of the model in predicting the behaviour of a structure subjected to dynamic excitations is not yet assessed.
In this paper the model is validated by comparing the theoretical results with those obtained by experiments carried out on a full scale structure endowed with HDR based dampers subjected to free vibration, displacement- controlled and force-controlled tests.

2. THE MOCK-UP

The mock up is a steel-concrete composite structure, consisting of a pair of one-storey two-bay moment resisting frames with a height of 3.00 m and spans of 4.20 m. The six columns are obtained with HE160A hot rolled grade S355 steel profiles. The composite beams are also obtained with HE160A grade S355 steel profiles and a 120 mm thick slab realised with C30/37 concrete cast on a collaborating EGB210 steel sheet. The composite slab is directly supported by the main beams and connected with Nelson studs in order to ensure full shear connection (Figs.1). The composite beam-to-column connections are partial-strength and are obtained by means of beam end-plates bolted to the column flange and by placing suitable reinforcements in the slab (Dezi et al. 2007). An additional mass of 12.4 *t* was placed on the slab thank to nine concrete blocks suitably linked to the structure in order to avoid undesired slides. The characterization of the bare frame, in the range of the elastic behaviour, was carried out by performing a series of snap back tests (Fig.2). Five levels of displacements were imposed below the elastic limit estimated for the frame. Table in Fig. 2 reports the values of frequencies, stiffness and damping ratios obtained for the bare frame. Both quasi-static (k_s) and dynamic (k_d) stiffness are reported, the first is deduced from the initial load path while the second is deduced from the frequency (assuming the total mass is known and equal to 26,6*t*). The damping coefficient ξ was deduced from the snap back tests by means of the classic logarithmic decrement method (Chopra 2000).

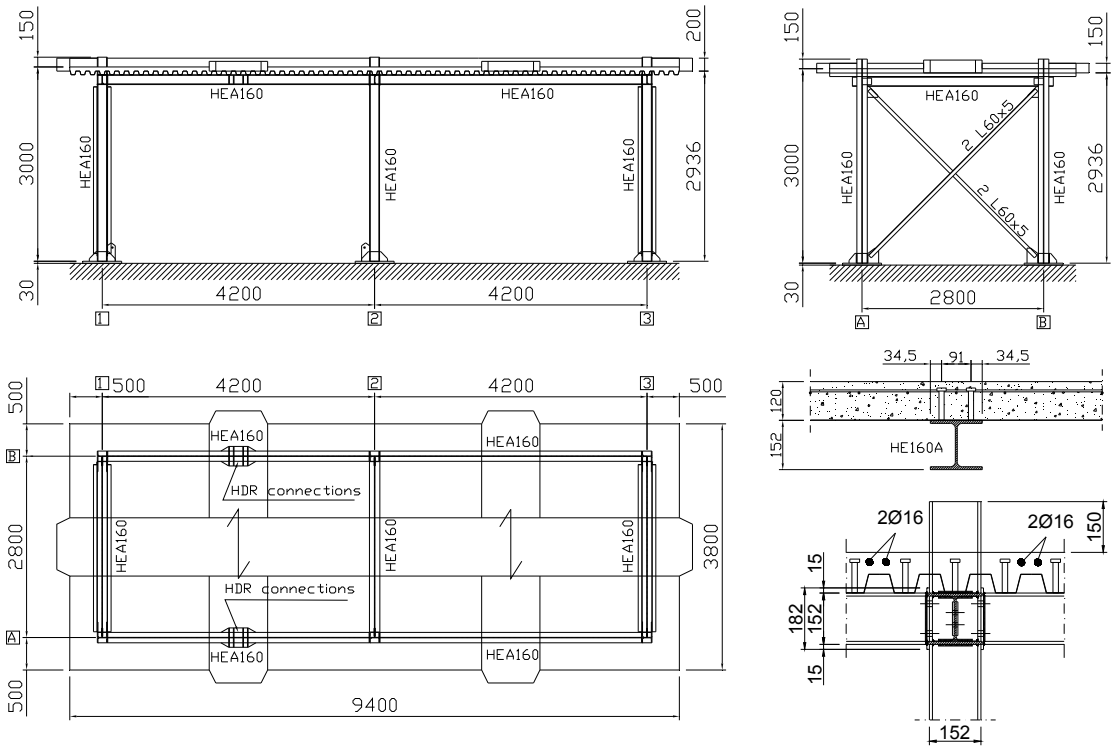

Figure 1 Steel-concrete composite mock-up

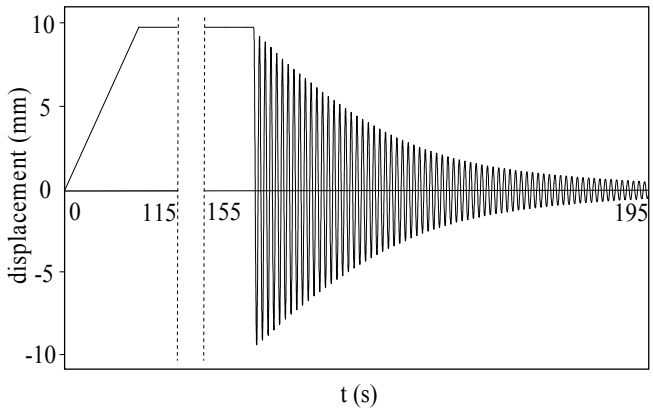

	Bare frame			
Displ. [mm]	Freq. [Hz]	k_s [kN/mm]	k_d [kN/mm]	ξ
2	2.78	8.67	8.10	0.004
4	2.76	8.43	7.98	0.005
6	2.72	7.99	7.80	0.006
8	2.70	7.71	7.67	0.006
10	2.68	7.50	7.53	0.006

Figure 2 Free vibration tests on the mock-up

3. TEST SET-UP

The dissipaters adopted are based on High Damping Rubber (HDR) and they are manufactured by T.A.R.R.C. (Tun Abdul Razak Research Center). The single device consists of two 170 x 230 x 5 mm superimposed rubber layers separated by an intermediate 2 mm thick steel shim. This was coupled with the frame by means of Chevron-type braces placed in the interior of the main moment resisting frames as shown by Figures 3. The dampers were placed horizontally and were directly bolted to the bottom flange of the steel beams and braces so as to undergo shear strain under the deck drift. In order to make the bracing system rigid with respect to the frame, and prevent undesirable movements between the frame and the dampers, the braces were stiffened by two prestressed cross-rods.

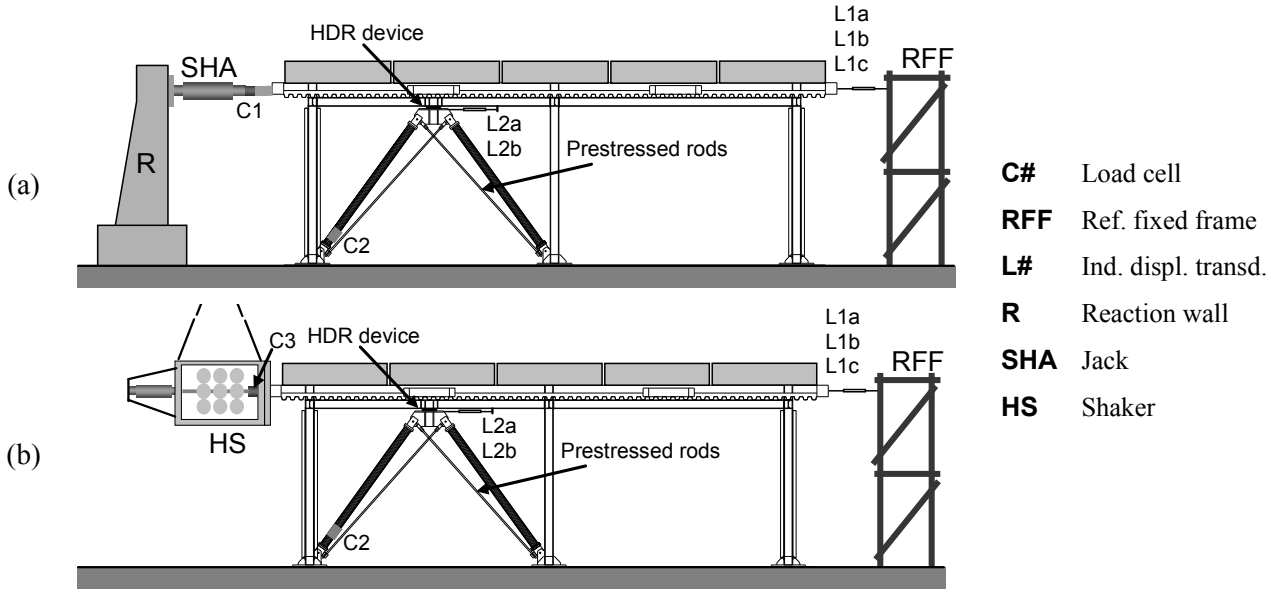

Figure 3 Test set-ups: (a) displacement-controlled tests; (b) force-controlled cyclic tests

The mock-up was instrumented so as to measure global forces and displacements of the frame as well as the local forces and strains in the HDR devices. In the case of free vibration tests and displacement-controlled cyclic tests, an actuator fixed to a reaction structure (R) was used to apply the displacements. The actuator is a 400 kN (±100 mm) servo-controlled hydraulic jack (SHA) and was placed in series with a load cell (C1) which measures the global forces as shown by Figure 3a. In the case of the force-controlled dynamic cyclic test, an electro-hydraulic shaker (HS) consisting of a mobile mass of 0.9 *t*, a displacement actuator of 100 *kN* (±100 *mm*) and a load cell (C3) were used, as shown by Figure 3b.

In all cases three inductive displacement transducers (L1a,b,c) were used to measure the storey drift opposite the actuators. One was placed at the centre and two at the edges of the slab in order to measure possible slab deformations and torsional rotations. Strains in the HDR devices were determined by measuring the relative displacements between the plates bolted to the frame and brace (L2a,b) while a load cell (C2) was mounted on one of the brace struts. The force acting on the HDR device was obtained by a correlation factor calculated by supposing the brace to have linear elastic behaviour.

4. ANALYTICAL MODEL OF THE COUPLED FRAME

Since the tests are performed within the elastic displacement range of the mock-up and the slab is expected to be in-plane stiff, the dynamic system constituted by the frame and the devices can be viewed as a SDOF in which two parallel resisting mechanisms take place. A linear spring and a dashpot represent the bare frame contribution whereas a non-linear viscoelastic device represents the dampers. The system is governed by the equation

$$m\ddot{u}(t) + 2\xi\sqrt{km}\,\dot{u}(t) + ku(t) + f_d(t) = f(t) \tag{4.1}$$

where f(t) is a generic external force and f_d is the restoring force provided by the HDR devices (Dall'Asta and Ragni 2008a,b), which may be written as

$$f_d = \beta\tau(\gamma, \dot{\gamma}, \boldsymbol{\alpha}) \tag{4.2}$$

where τ and γ are the shear stress and strain, respectively, acting on the rubber and β is a multiplier factor, which has to be experimentally calibrated, that depends on the rubber area and takes into account secondary phenomena (such as brace deformations or slips at the connections, etc.). Obviously Eqn. 4.1 has to be considered in conjunction with the equations describing the evolution of the rubber internal variables. A numerical solution of the problem may be easily obtained by means of Runge-Kutta method once the vector of the state ($\boldsymbol{\chi}$) is introduced

$$\boldsymbol{\chi}^T = \begin{bmatrix} u & v & \boldsymbol{\alpha}^T \end{bmatrix} \tag{4.3}$$

which groups displacement and velocity of the mass and the five internal variables of the rubber devices (vector $\boldsymbol{\alpha}$). Eqn. 4.1 may be rewritten accounting for the evolution laws of the rubber as

$$\dot{\boldsymbol{\chi}} + \mathbf{C}\boldsymbol{\chi} + \mathbf{f}_d(\boldsymbol{\chi}) = \mathbf{f} \tag{4.4}$$

where

$$\mathbf{C} = \begin{bmatrix} 0 & -1 & 0 \\ \dfrac{k}{m} & \dfrac{c}{m} & 0 \\ 0 & 0 & 0 \end{bmatrix} \qquad \mathbf{f}_d{}^T = \begin{bmatrix} 0 & \dfrac{\beta\tau\left(\dfrac{u}{h}, \dfrac{v}{h}, \alpha\right)}{m} & -\mathbf{A}^T\left(\dfrac{u}{h}, \dfrac{v}{h}, \alpha\right) \end{bmatrix} \qquad \mathbf{f}^T = \begin{bmatrix} 0 & f & 0 \end{bmatrix} \tag{4.5}$$

and h indicates the thickness of the rubber used in the dissipation devices. The parameters of the bare frame (k and ξ) appearing in Eqn. 4.5 are evaluated from experimental test carried out on the bare frame and they are k = 8.0 kN/mm and ξ = 0.006, while the mass m = 26.6 t was estimated from the geometry of the structure. The parameters of the HDR based devices are evaluated by experiments carried out on the single device (Dall'Asta and Ragni 2006), whereas the multiplier factor β was obtained directly from the signal of the load cell C2, which measures the force acting in the braces.

4. VALIDATION OF THE HDR MODEL

4.1. Snap back tests

The snap back tests described in section 2 were also performed on the frame equipped with the HDR dissipating devices. Figure 4 reports the displacement histories obtained by imposing different initial displacements. It is evident that the system behaviour strongly depends on the displacement amplitude: this is more and more stiff as the displacements decrease. Finally, since the rubber is a fading memory material, in all cases the displacement goes to zero in a sufficiently short period of time. In order to compare the results observed in the bare frame (almost linear) with those of the equipped frame (strongly nonlinear) the values of the frequencies, quasi-static and dynamic stiffness and damping ratios are reported by the table in Figure 4. In this case the values of frequencies and dynamic stiffness were obtained by considering the average of the values observed in the first two oscillations. The damping coefficient ξ was deduced by means of the logarithmic decrement method (Chopra 2000), as in linear systems, considering only the first two oscillations. The values of stiffness and damping obtained are much higher with respect to those of the bare frame, confirming the stiffness and the large dissipation capacity of the rubber devices.

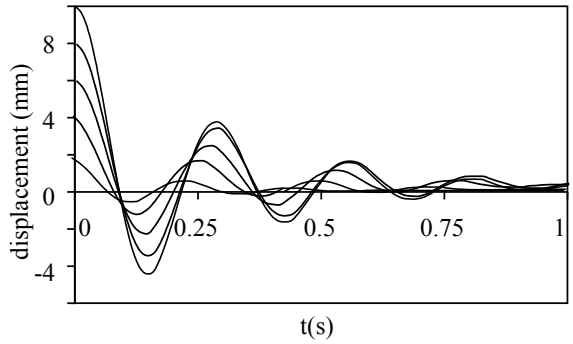

	Equipped frame (mean values)			
Displacement [mm]	Frequency [Hz]	k_s [kN/mm]	k_d [kN/mm]	ξ
2	4.61	14.87	22.37	0.23
4	4.06	12.98	17.28	0.18
6	3.94	12.49	16.34	0.16
8	3.66	11.63	14.04	0.14
10	3.57	11.77	13.39	0.13

Figure 4 Snap-back of the equipped frames

Snap-back tests are numerically simulated starting from natural conditions $\chi(0)=\mathbf{0}$, by imposing the initial displacement path and performing the subsequent free vibration analysis. The results of the numerical simulation and the experimental test are compared in Figure 5, with reference to the initial 10 mm displacement. They are in good agreement, confirming the ability of the HDR model proposed in simulating the dynamic response of the coupled system.

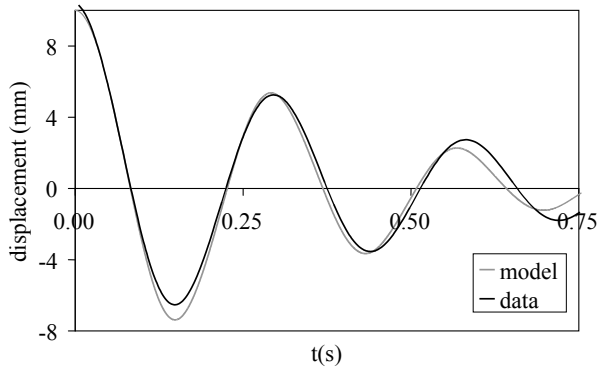

Figure 5 Experimental and numerical displacement histories of the snap-back test

4.2 Force-controlled cyclic tests

The second set of tests performed were force-controlled cyclic tests. They were carried out by means of an electro-hydraulic shaker in order to investigate the structure's behaviour in a wide range of frequencies and force amplitudes. The electro-hydraulic shaker was suspended and anchored to the structure. It consists of a

servo-controlled hydraulic actuator and a 0.9 *t* mobile mass to which a sinusoidal displacement is imposed. In particular the software used to control the shaker can impose frequency sweeps, by varying in continuum the frequency of the external force and modifying, at the same time, the stroke of the actuator so that the external force amplitude remains constant.
The test procedure was divided into two steps. The first step consisted of imposing rising and descending frequency sweeps in order to identify the resonance condition (Figure 6). Successively cyclic tests at fixed frequency values, including the resonance frequency, were performed. This procedure was repeated for different force amplitudes (from 3 kN to 9 kN) in order to investigate the non linear behaviour of the system due to the HDR dissipation devices. The frequency range investigated depends on the limits of the hydraulic system and consequently varies for the different force intensities.

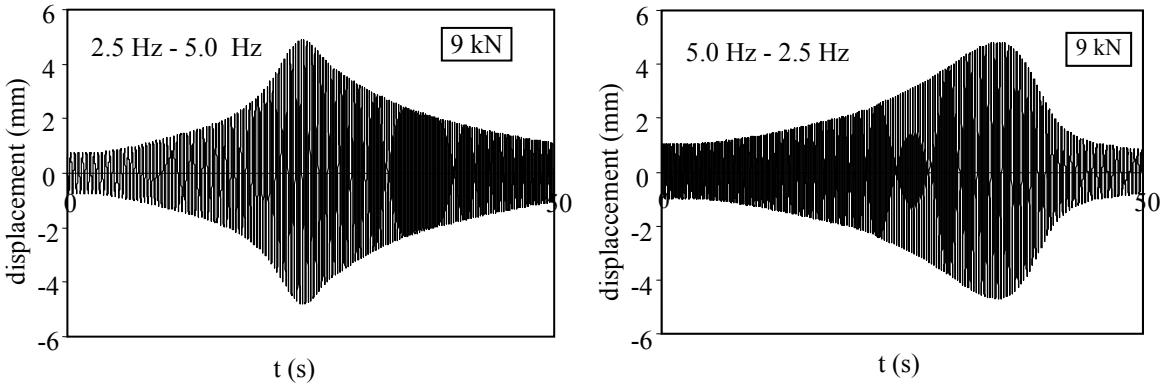

Figure 6 Displacement time histories of rising sweep and descending sweeps.

Figure 7a shows maximum displacement vs. frequency diagrams for different force amplitudes. It may be observed that the maximum displacement increases nonlinearly and the resonance frequency decreases for increasing force amplitudes. This is due to the softening behaviour of the rubber in the displacement range investigated. Furthermore, Figure 7b shows the force-displacement diagram of the devices at the resonance conditions at different force levels. These diagrams point out the softening behaviour of the rubber, due to the different strain amplitudes, as well as to the different strain rates of the tests performed at the resonance conditions.

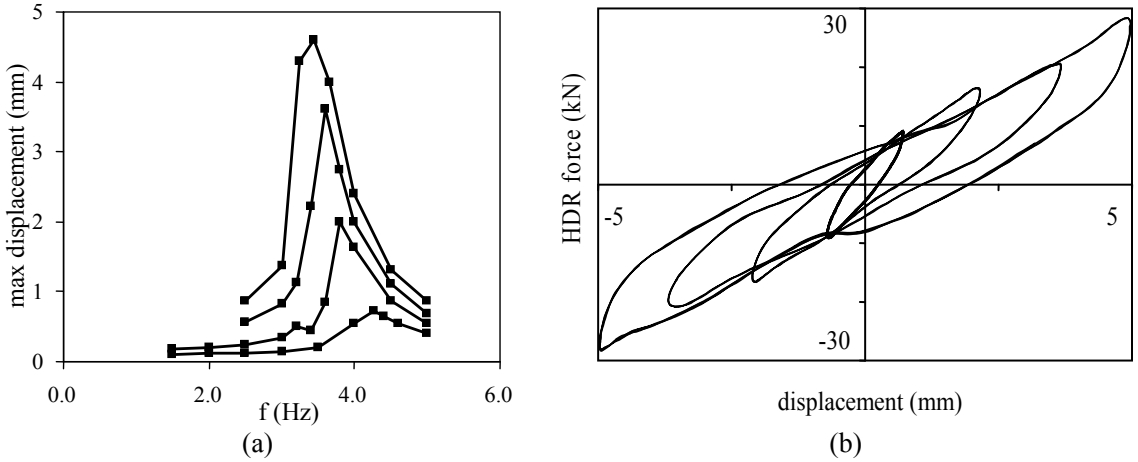

Figure 7 Maximum displacement vs. frequency diagram (a); force-displacement diagrams of the devices (b).

The force-controlled cyclic tests were also simulated. In this case the initial conditions are null, while the external force is $f_e(t) = f_0 \sin \omega t$, where f_0 is the amplitude and ω the circular frequency. Figure 8 shows a comparison between the maximum displacement vs. frequency diagrams experimentally obtained and those obtained by the numerical simulation. Figure 9 reports the simulation of the force-displacement diagrams of the dissipation

devices at resonance conditions for force amplitudes equal to 3 kN and 9 kN. Also in this case experimental and numerical results are in good agreement.

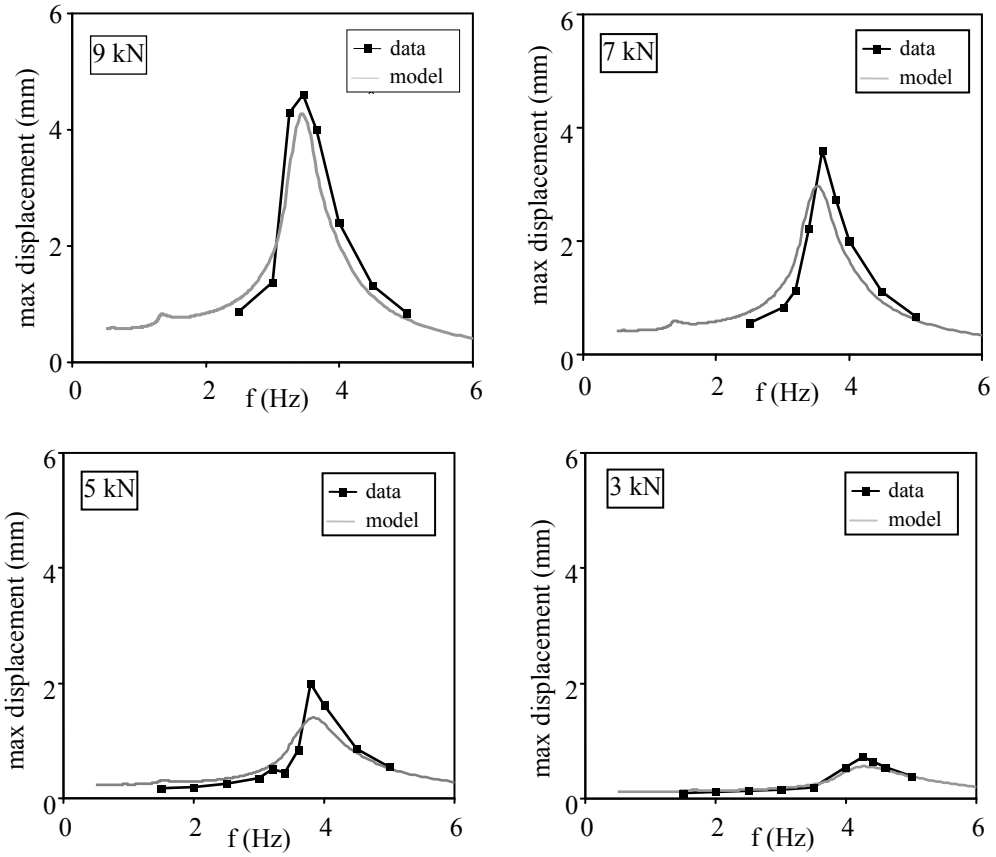

Figure 8 Experimental and numerical results of force-controlled cyclic tests

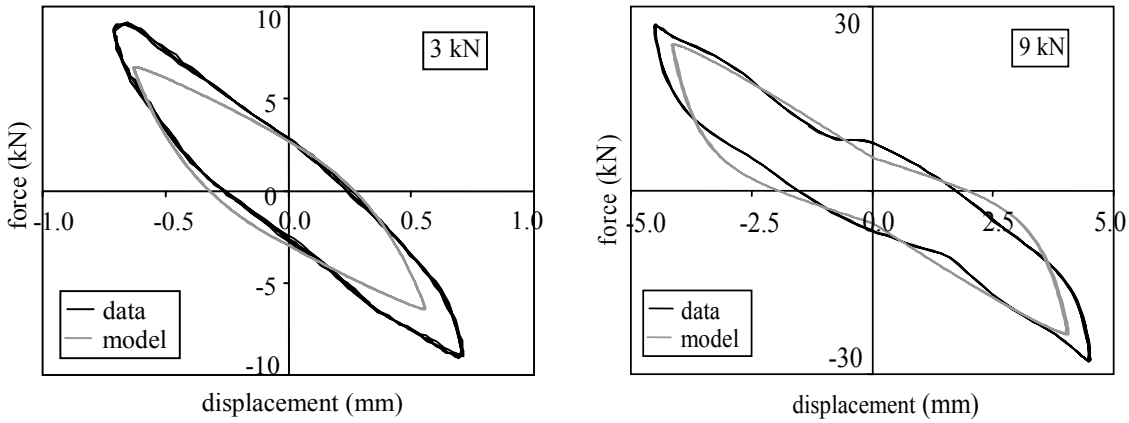

Figure 9 Force-displacement diagrams of the dissipation devices

4.3 Displacement-controlled cyclic tests

Displacement-controlled cyclic tests were performed in order to study the behaviour of the coupled system with increasing and decreasing displacements at a fixed frequency. Only low frequencies may be applied because of the dimensions of the system tested and the limits of the hydraulic system and of the reaction structure. In particular, the test consisted of a sinusoidal imposed displacement path with constant frequency 0.5 Hz. The amplitude of the cycles was increased from 2 to 8 mm and then decreased from 8 to 2 mm by steps of 2 mm. Each variation of the amplitude was imposed after 6 constant cycles with one transient cycle (Fig.10a).

Unlike the tests previously described, where the displacements of the system are a consequence of the initial imposed conditions or of the imposed force histories, here the displacements are directly imposed to the system, consequently, in the numerical simulation, the history of the displacement $\bar{u}(t)$ and the velocity $\bar{v}(t)$ are known and the total force f may be straightforward computed by substituting the displacement and velocity histories in Eqn. 4.4. Comparisons with experimental data are in good agreement, as shown by Figure 10b.

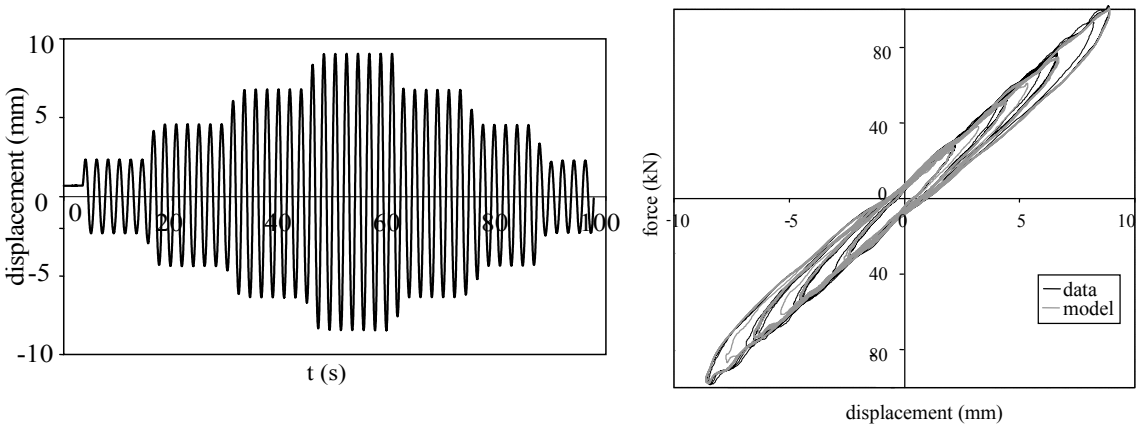

(a) (b)

Figure 10 Displacement time history (a); total force-displacement diagram (b).

ACKNOWLEDGMENTS

The study presented in this paper was developed in the framework of the ReLUIS National Research Project. Support from the ReLUIS-DPC, Italian University Network of Seismic Engineering Laboratories and Italian Civil Protection Agency, is gratefully acknowledged.

REFERENCES

Chopra A.K. (2000). Dynamics of Structures: Theory and Applications to Earthquake Engineering. Prentice-Hall, Upper Saddle River, NJ, (2nd Ed.).

Dall'Asta A. and Ragni, L. (2006). Experimental tests and analytical model of High Damping Rubber dissipating devices. *Engineering Structures*, **28**, 1874-1884.

Dall'Asta A. and Ragni L. (2008a). Dynamic systems with high damping rubber: nonlinear behaviour and linear approximation. *Earthquake Engineering and structural dynamics*. DOI:10.1002/eqe.825.

Dall'Asta A. and Ragni L. (2008b). Nonlinear behaviour of dynamic systems with high damping rubber. *Engineering Structures*,DOI:10.1016/j.engstruct,2008.06.003.

Dezi L., Giacchetti R., Ragni L., Zito L., Dall'Asta A., Leoni G. (2007). Application of HDR Devices for the Seismic Protection of Steel Concrete Composite Frames: Experimental Results. *Atti XII Convegno ANIDIS*.

Fuller K., Ahmadi H., Goodchild I., Magonette G., Taucer F. and Dumoulin C. (2000). Rubber-based energy dissipators for earthquake protection of structures. *Proceedings of the 12th WCEE,* Oakland, New Zealand.

Grant D.N., Fenves G.L. and Auricchio F., 2005. Modelling and Analysis of High-damping Rubber Bearings for the Seismic Protection of Bridges, Iuss Press, Pavia.

Haupt P. e Sedlan H. (2001). Viscoplasticity of elastomeric materials: experimental facts and constitutive modelling. Arch. Appl. Mech.,**71**, 89-109.

Hwang J.S., Wu J.D., Pan T.-C. and Yang G.. A (2002). A mathematical hysteretic model for elastomeric isolation bearings. *Earthquake Engineering and Structural Dynamics*, **31:4**, 771-789.

Soong T.T. and Spencer B.F. (2002). Supplemental energy dissipation: state-of-the art and state-of- the practice. *Engineering Structure*, **24**, 243-259.

Tsai C.S., Chiang T.-C., Chen B.-J. and Lin S.-B. (2003). An advanced analytical model for high damping rubber bearings. *Earthquake Engineering and Structural Dynamics*, **32:9**, 1373-1387.